Characterising Viral Vectors for Gene Therapy Delivery Using Mass Spectrometry on Different Levels

Josh Smith¹, Corentin Beaumal¹, Silvia Millán-Martín¹, Sara Carillo¹, Aaron Richardson¹, Colin Clarke^{1,2} & Jonathan Bones^{1,2}

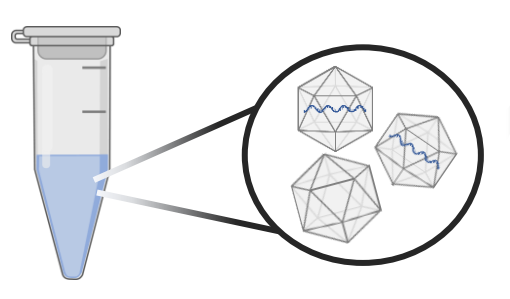
¹NIBRT, Foster Avenue, Mount Merrion, Blackrock, Co. Dublin, A94 X099, Ireland.

²School of Chemical and Bioprocess Engineering, University College Dublin, Belfield, Dublin 4, D04 V1W8, Ireland.



Capsid Fill State Assessment Using Native MS



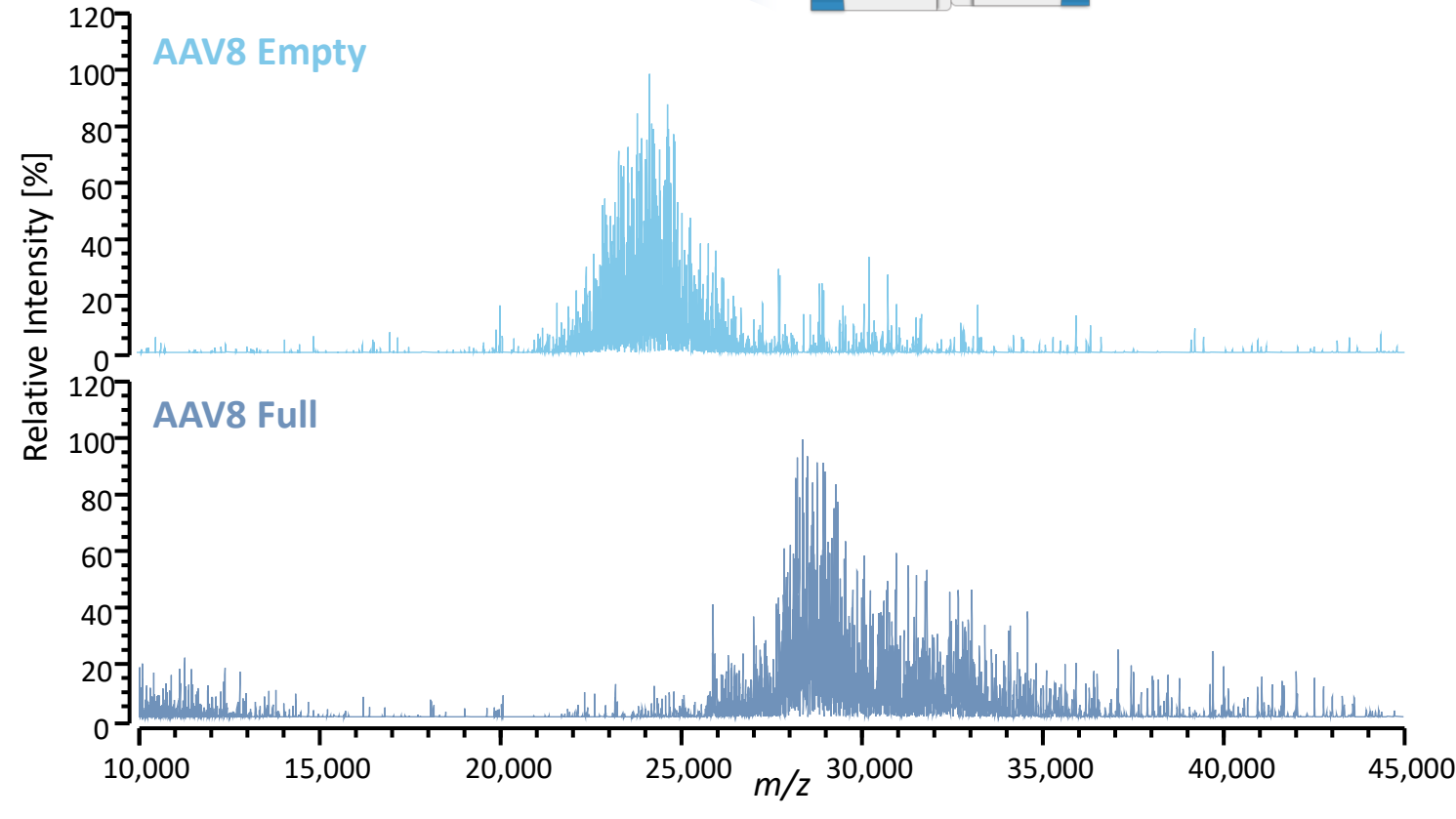


Buffer exchange or dilute sample

Direct infusion *via* static nanoESI

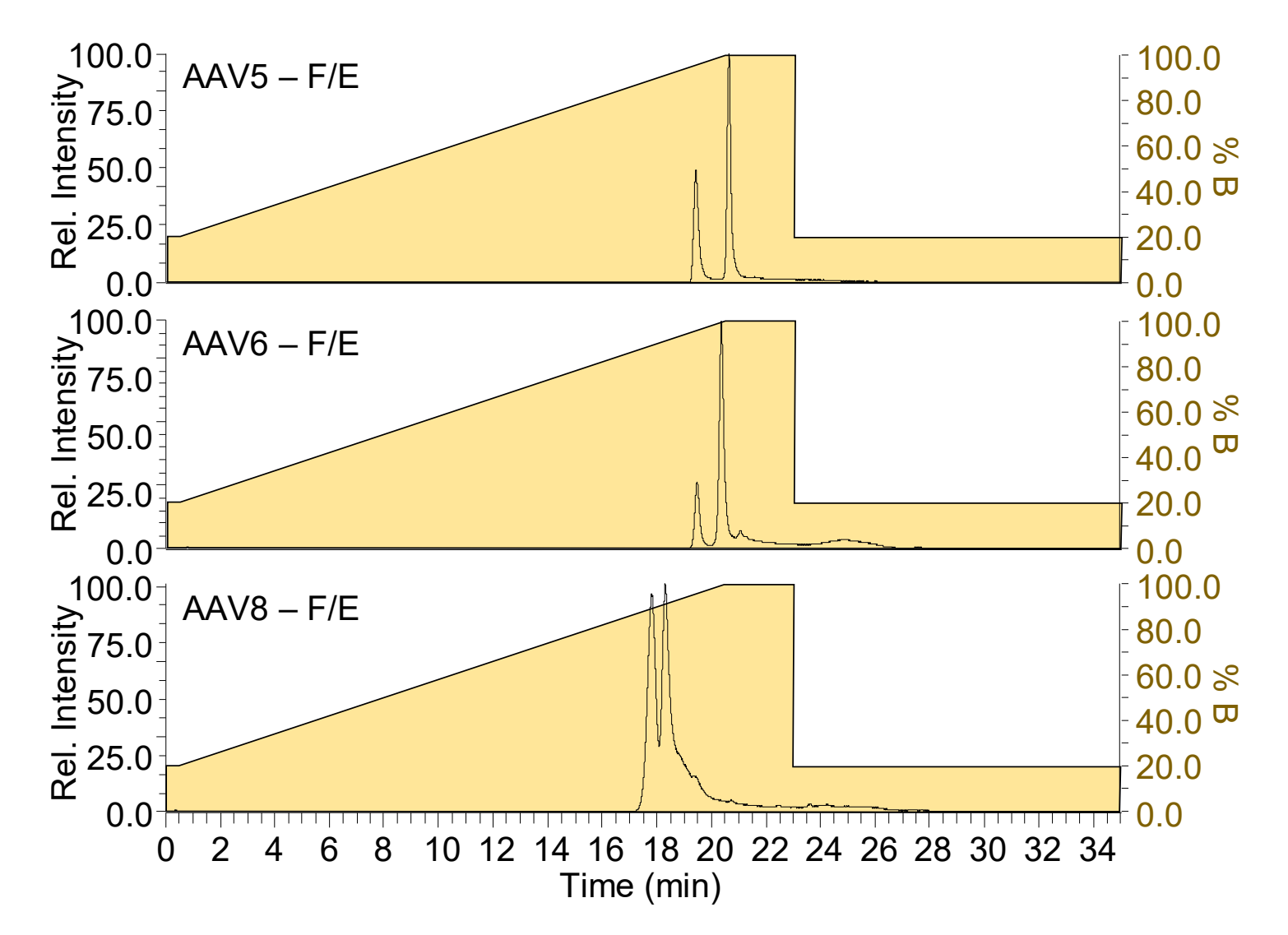


Thermo Q Exactive UHMR	Setting								
Resolution	25,000 at m/z 200								
Microscans	10								
AGC Target	1e06								
Max. IT	200 ms								
In-source trapping	-100 V								
Source DC offset	-50 V								
Extended trapping	150 V								
Trapping gas	SF ₆ at 4e-10 mbar								
Acquisition	5 mins with transient averaging enabled								



Coupling with Anion Exchange Chromatography

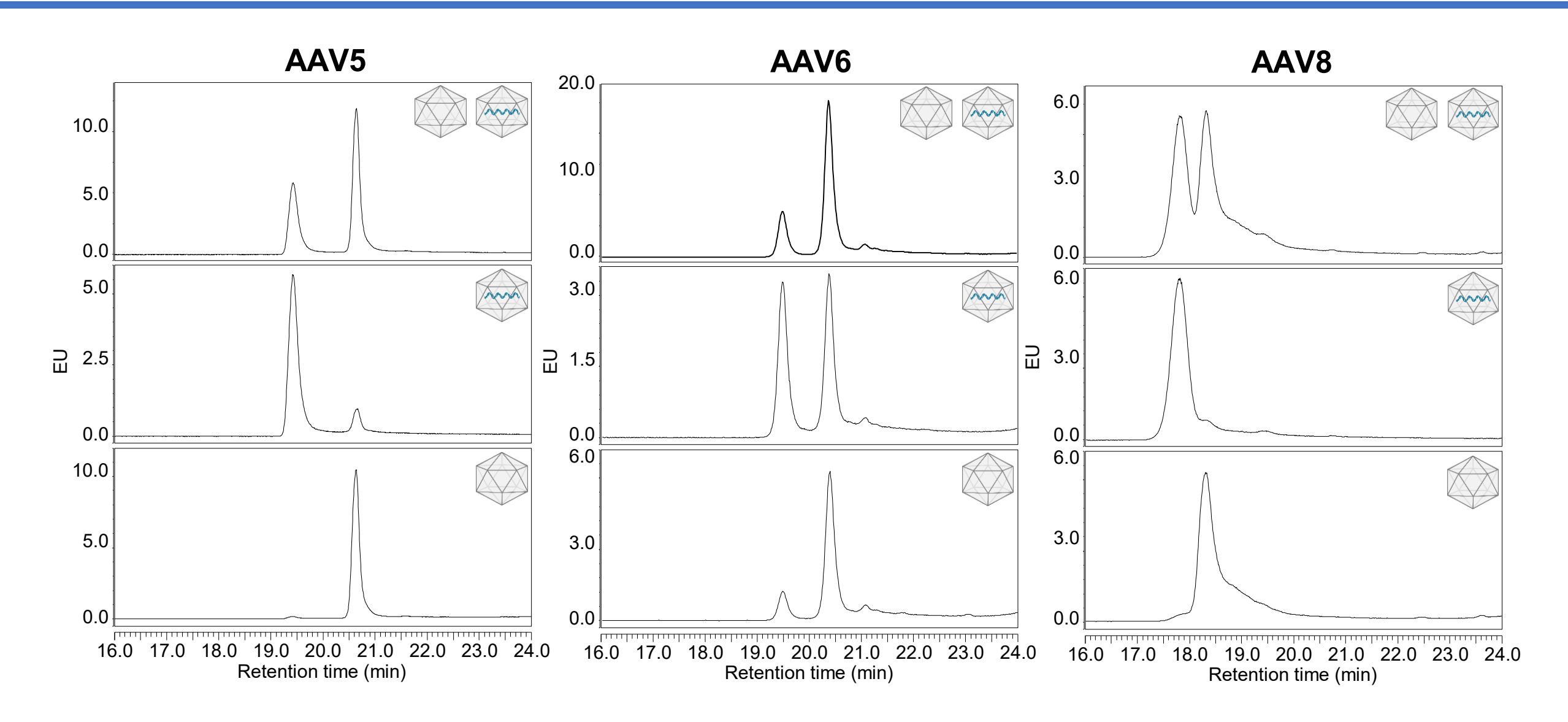




- pH gradient anion exchange separation of full and empty capsids using Thermo Scientific ProPac 3R AEX column.
- Gradient specifically designed to be generic for different serotypes and mass spectrometry compatible.
- pH gradients enable focusing effect, elution occurs when gradient pH = analyte pl, results in sharp chromatographic peaks.

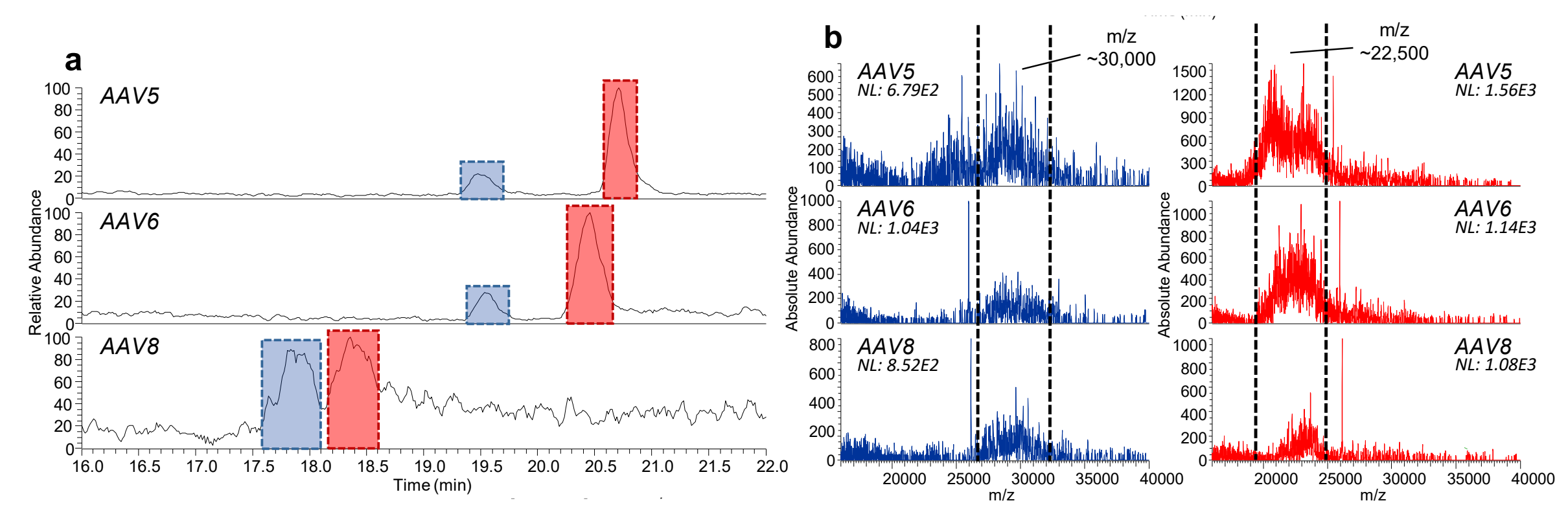
Determination of Capsid Fill State Elution Order





Coupling pH Gradient AEX with Native MS Detection

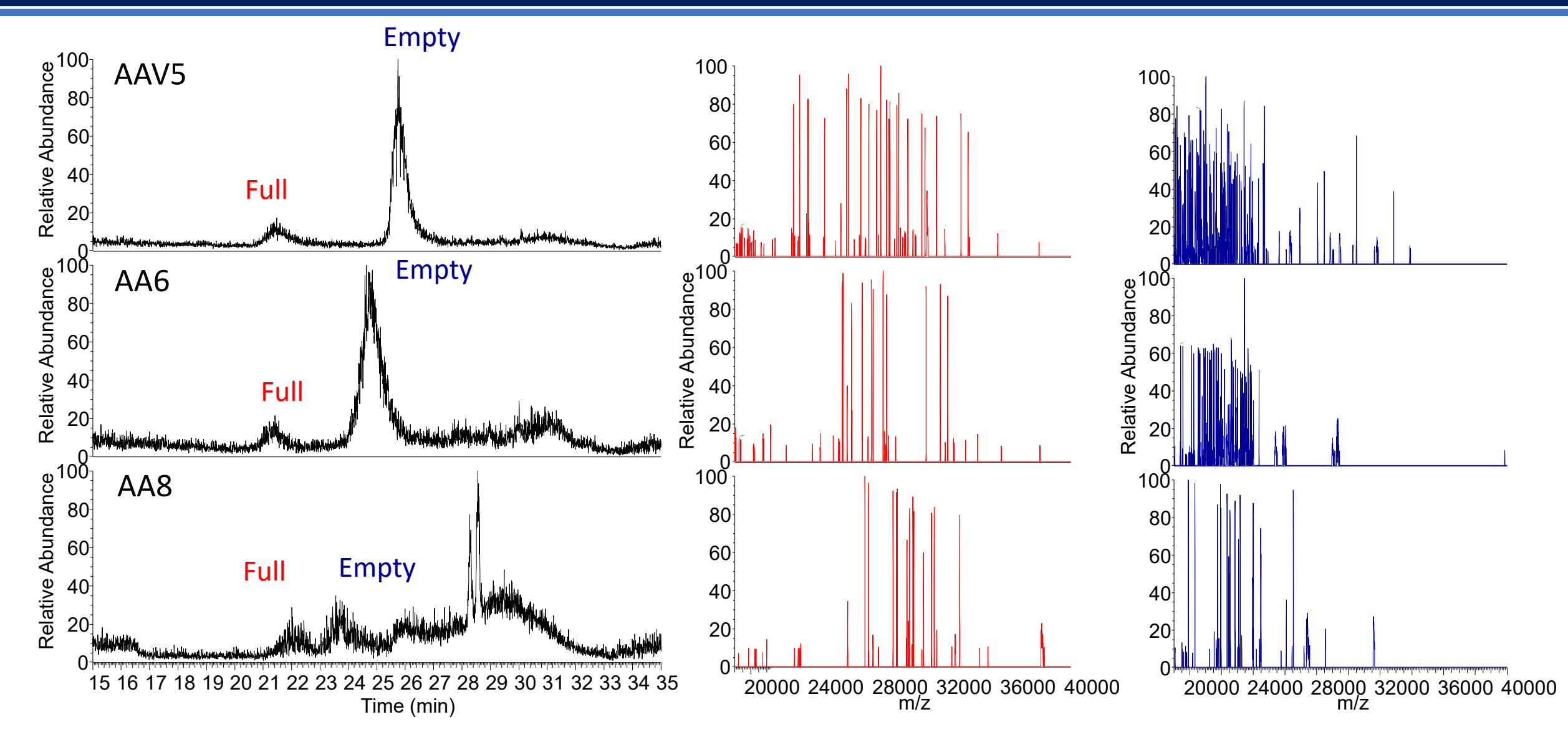




- □ pH gradient anion exchanged coupled directly to Thermo Scientific Q Exactive UHMR mass spectrometer for confirmation of capsid fill state species identification based on m/z.
- Assuming similar charge, earlier eluting peak contains heavier species explained by the presence of cargo DNA, additional mass of ~0.8 MDa corresponding to CMV-GFP.

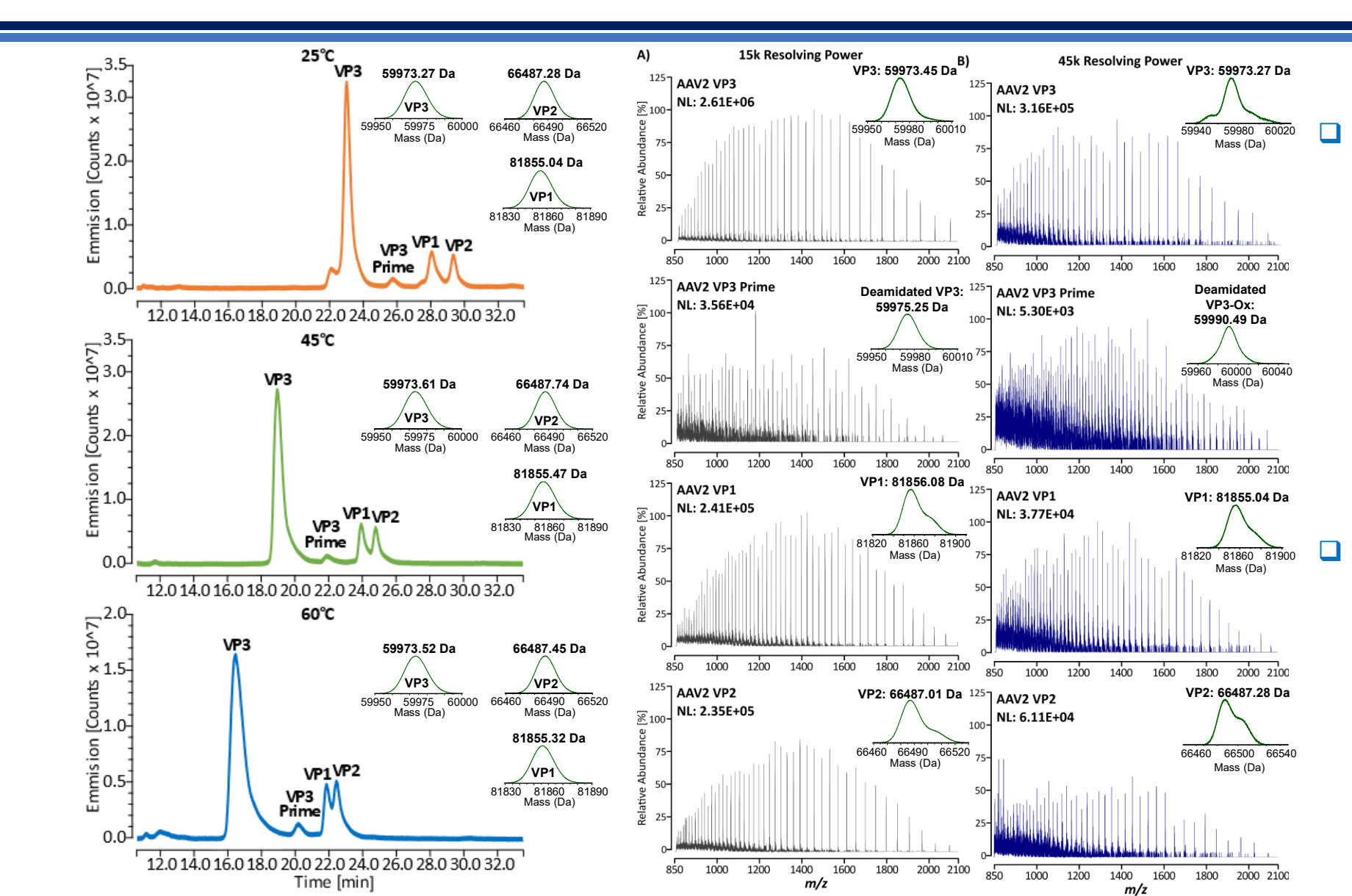
Coupling pH Gradient AEX with Charge Detection MS





Viral Protein Separation using LC-MS





VP separation using hydrophilic interaction LC using an acetonitrile water gradient containing difluoro acetic acid as a mobile phase modifier.

Fluorescence and MS detection using Thermo Scientific Orbitrap Exploris 240 MS with Biopharma Option.

Method Translation into Rapid Identity Test

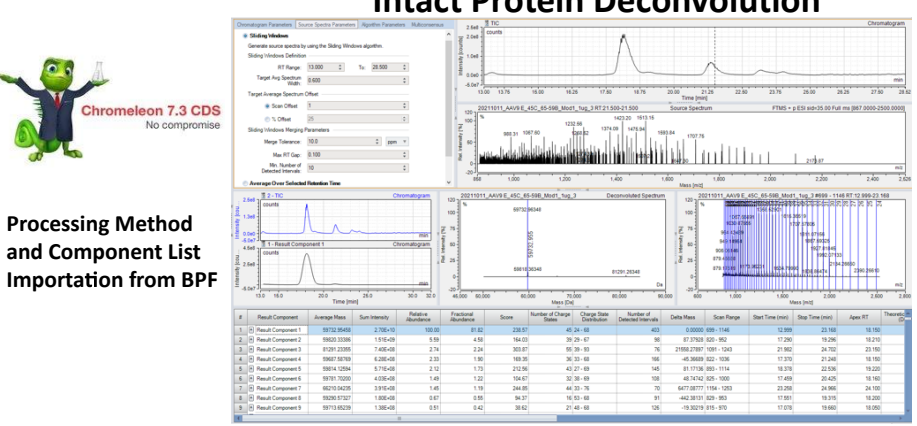




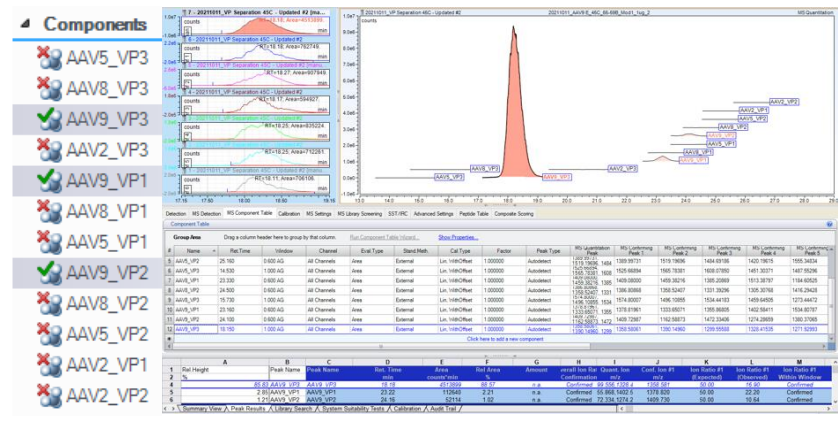


BioPharma Finder Software 4.1

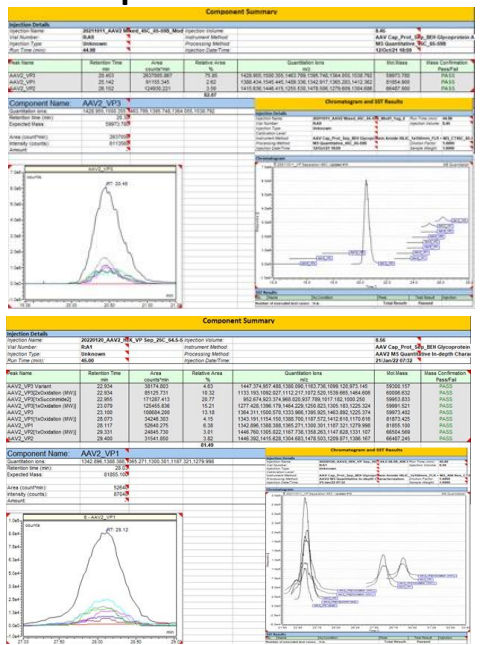
Intact Protein Deconvolution



Data Processing Parameter Optimization (Sf9 Derived AAVs)



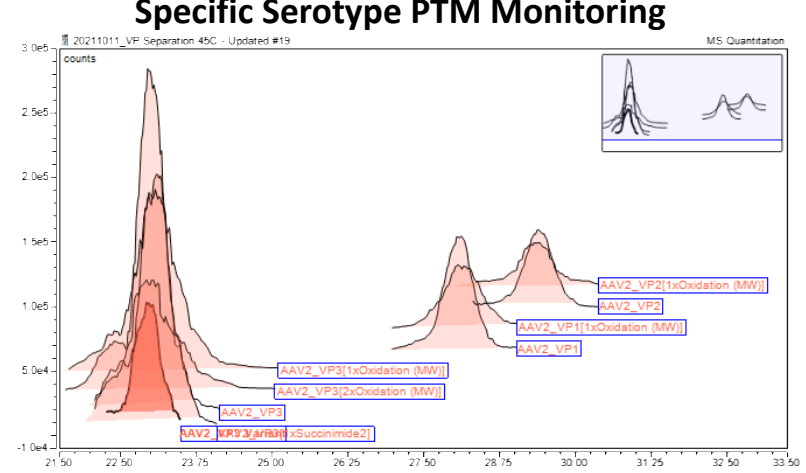
Report Generation



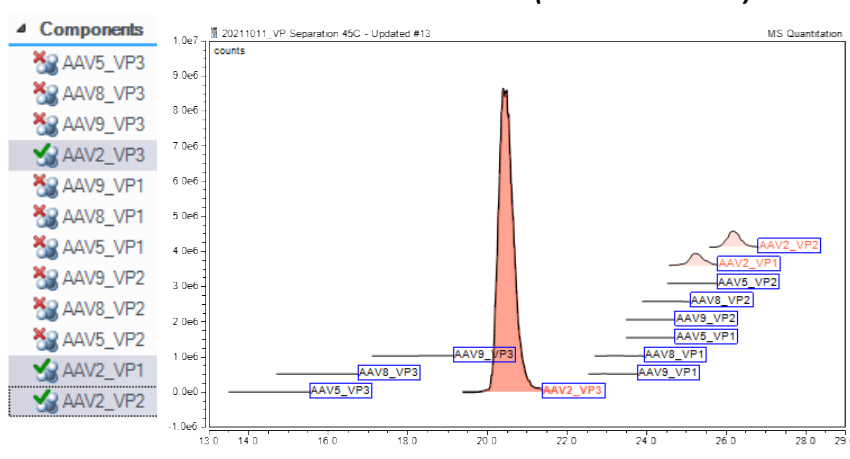
Specific Serotype PTM Monitoring

Serotype

Profiling

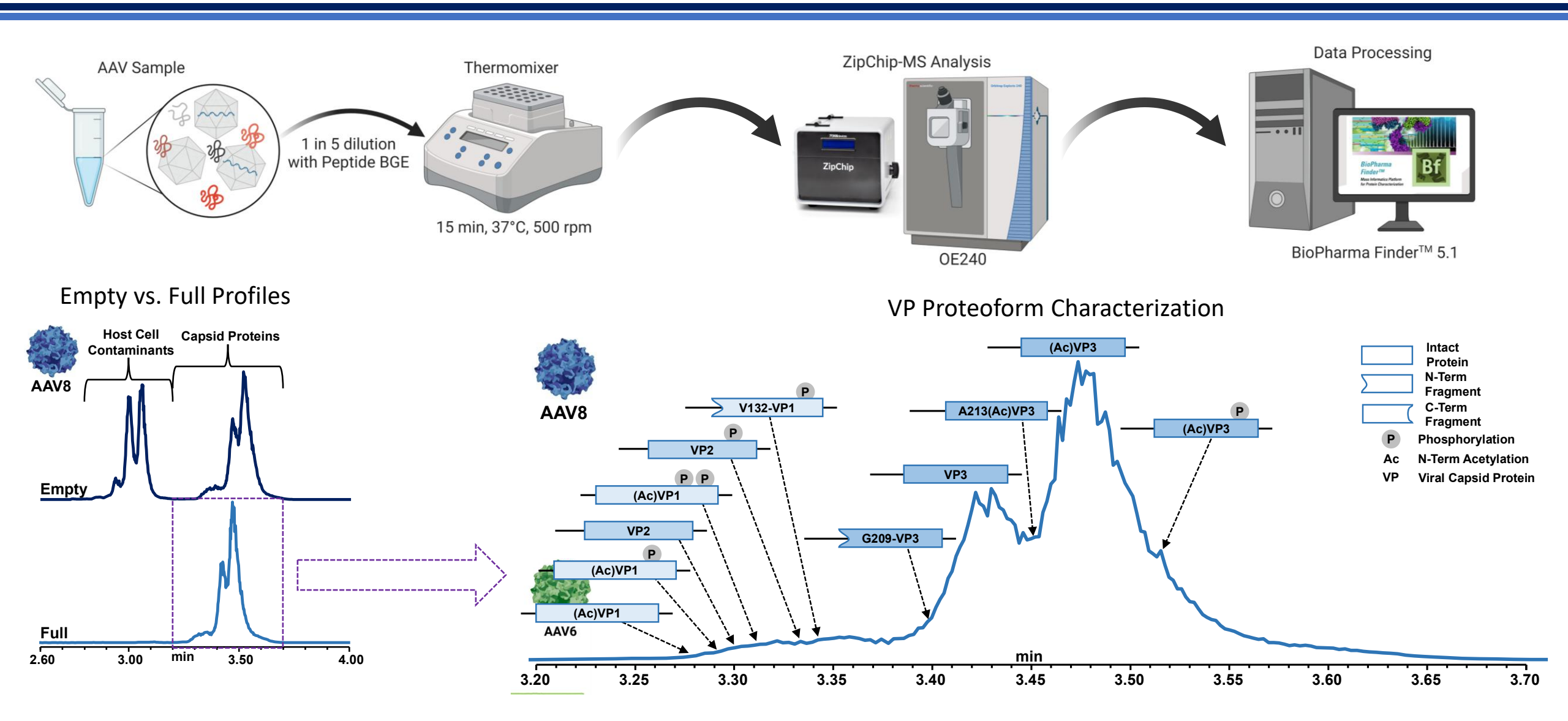


Method Validation (HEK Derived AAV)



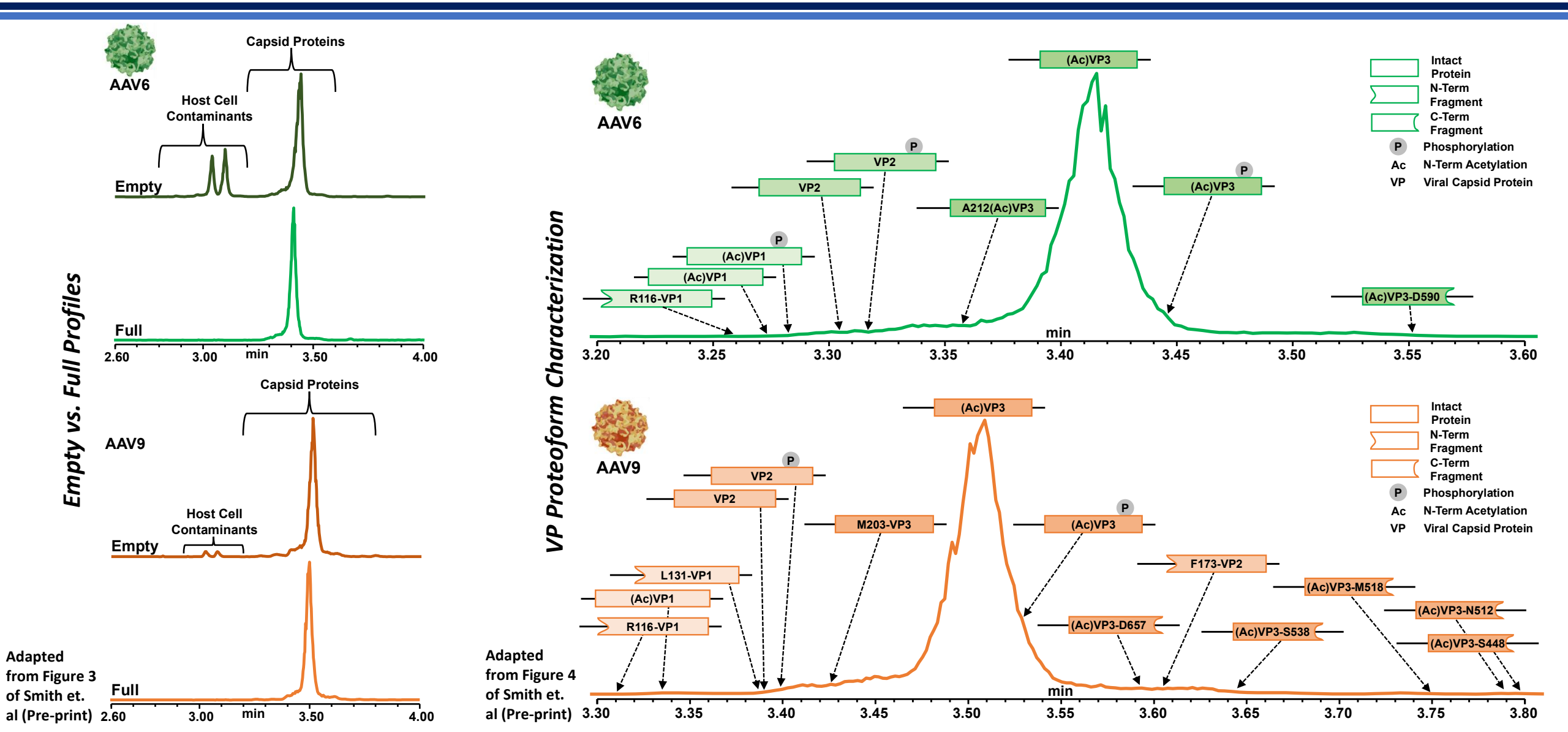
Viral Protein Separation using MCE-MS





Broad Applicability of ZipChip Platform





Detected VP Proteoforms and Fragments



Start of AAV Sequence

-►VP1 **AADGYLPDWLEDTLSEGIRQWWKLKPGPPPPKPAERHKDDSRGLVLPGY** KYLGPFNGLDKGEPVNEADAAALEHDKAYDRQLDSGDNPYLKYNHADAEF QERLKEDTSFGGNLGRAVFQAKKRVLEPLGLVEEPVKTAPGKKRPVEHSP 100 **VEPDSSSGTGKAGQQPARKRLNFGQTGDADSVPDPQPLGQPPAAPSGLGT** 150 ı-►VP3 ı-▶ A211-VP3 NTMATGSGAPMADNNEGADGVGNSSGNWHCDSTWMGDRVITTSTRTWALP 200 203 249 TYNNHLYKQISSQSGASNDNHYFGYSTPWGYFDFNRFHCHFSPRDWQRLI 250

VP3 Variant Generation

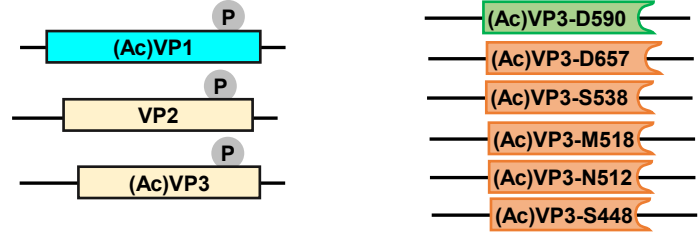
Serotypes	N-terminal region										DP	sec	que	nce	DG	se	que	nce	DP sequence						
Colotypes		203								211			590	591			626	627				656	657		
AAV1		M	Α	S	G	G	G	Α	Р	M	Α	 Т	D	Р	Α	 Т	D	G	Н		Α	N	Р	Р	
AAV2		M	Α	Т	G	S	G	Α	Р	M	Α	 R	Q	Α	Α	 Т	D	G	Н		Α	Ν	Ρ	S	
AAV3		М	Α	S	G	G	G	Α	Р	М	Α	 Т	Α	Ρ	Т	 Т	D	G	Н		Α	Ν	Ρ	Ρ	
AAV6		М	Α	S	G	G	G	Α	Р	M	Α	 Т	D	P	Α	 Т	D	G	Н		Α	Ν	Ρ	Ρ	
AAV8		М	Α	Α	G	G	G	Α	Р	M	Α	 Т	Α	Ρ	Q	 Т	D	G	Ν		Α	D	P	Р	
AAV10		M	Α	Α	G	G	G	Α	Р	М	Α	 Т	G	Ρ	Ι	 Т	D	G	Ν		Α	D	Р	Р	
AAVrh10		М	Α	Α	G	G	G	Α	Р	M	Α	 Α	Α	Ρ	Ι	 Т	D	G	Ν		Α	D	Р	Р	
AAV4		M	R	Α	Α	Α	G	G	Α	Α	V	 Ν	L	Ρ	Т	 Т	D	G	Н		Α	Ν	Ρ	Α	
AAV11		M	R	Α	Α	Р	G	G	Ν	Α	V	 Т	Α	Ρ	Ι	 Α	D	G	Н		Α	Ν	Ρ	Α	
AAV12		M	R	Α	Α	Р	G	G	Ν	Α	V	 Т	Α	Ρ	Н	 Т	D	G	Н		Α	Ν	Р	Ν	
AAV5		M	S	Α	G	G	G	G	Р	L	G	 Т	Α	Ρ	Α	 Т	G	Α	Н		G	Ν	1	-	
AAV9		M	Α	S	G	G	G	Α	Р	V	Α	 Α	Q	Α	Q	 Т	D	G	Ν		Α	D	Ρ	Р	
AAV7		V	Α	Α	G	G	G	Α	Р	M	Α	 Т	Α	Α	Q	 Т	D	G	Ν		Α	Ν	Ρ	Ρ	

Adapted from Figure 5a of Oyama et al. (2021) https://www.liebertpub.com/doi/10.1089/hum.2021.009

							•	/ 1	_	_	ı.		,,	_	_	.	_	_	c	_		_	_:		_								
				Firs	-		_	<u></u>	<u>e</u>	<u>u</u>	<u>K</u>	<u> </u>		<u>_</u>	<u>U</u>	<u> </u>	<u> </u>	<u> </u>	<u>၁</u>	<u> </u>	aı	<u> 111</u>	<u> 11</u>	<u> </u>	<u>g</u>		Se	100	nd				
		ini	tiati	on	coc	ion																				ını	uati	on (coa	on			
 Α	С	Α	Α	Т	G	G	С	Т	Т	С	Α	G	G	С	G	G	Т	G	G	С	G	С	Α	С	С	Α	Α	т	G	G	С	Α	•••
 Α	С	G	Α	т	G	G	С	Т	Α	С	Α	G	G	С	Α	G	Т	G	G	С	G	С	Α	С	С	Α	Α	T	G	G	С	Α	
 Α	С	Α	Α	т	G	G	С	Т	Т	С	Α	G	G	С	G	G	Т	G	G	С	G	С	Α	С	С	Α	Α	T	G	G	С	Α	
 Α	С	Α	A	т	G	G	С	Т	Т	С	Α	G	G	С	G	G	Т	G	G	С	G	С	Α	С	С	Α	Α	т	G	G	С	Α	
 Α	С	Α	A	т	G	G	С	Т	G	С	Α	G	G	С	G	G	Т	G	G	С	G	С	Α	С	С	Α	Α	Т	G	G	С	Α	
 Α	С	Α	A	т	G	G	С	Т	G	С	Α	G	G	С	G	G	Т	G	G	С	G	С	Т	С	С	Α	Α	т	G	G	С	Α	
 Α	С	Α	Α	т	G	G	С	Т	G	С	Α	G	G	С	G	G	Т	G	G	С	G	С	Т	С	С	Α	Α	Т	G	G	С	Α	
 G	Α	G	Α	т	G	С	G	Т	G	С	Α	G	С	Α	G	С	Т	G	G	С	G	G	Α	G	С	Т	G	С	Α	G	Т	С	
 G	Α	Α	A	т	G	С	G	Т	G	С	Α	G	С	Α	С	С	G	G	G	С	G	G	Α	Α	Α	Т	G	С	Т	G	Т	С	
 G	Α	G	A	т	G	С	G	Т	G	С	G	G	С	G	С	С	Α	G	G	С	G	G	Α	Α	Α	Т	G	С	Т	G	Т	С	
 Α	С	Α	A	Т	G	Т	С	Т	G	С	G	G	G	Α	G	G	Т	G	G	С	G	G	С	С	С	Α	Т	Т	G	G	G	С	
 Α	С	Α	Α	т	G	G	С	Т	Т	С	Α	G	G	Т	G	G	Т	G	G	С	G	С	Α	С	С	Α	G	Т	G	G	С	Α	
 Α	С	Α	G	т	G	G	С	Т	G	С	Α	G	G	С	G	G	Т	G	G	С	G	С	Α	С	С	Α	Α	т	G	G	С	Α	

Adapted from Figure S4a of Oyama et al. (2021) https://www.liebertpub.com/doi/10.1089/hum.2021.009 **Expected VPs N-Term Fragments** (Ac)VP1 R116-VP1 VP2 V132-VP1 (Ac)VP3 G209-VP3 VP3 Variant R116-VP1 L131-VP1 A212(Ac)VP3 A213(Ac)VP3 F173-VP2

VPs with additional PTMs C-Term Fragments



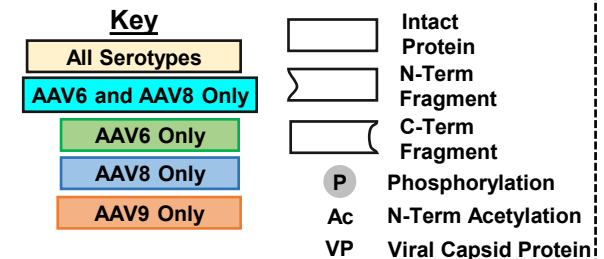
Unexpected VPs VP3

M203-VP3

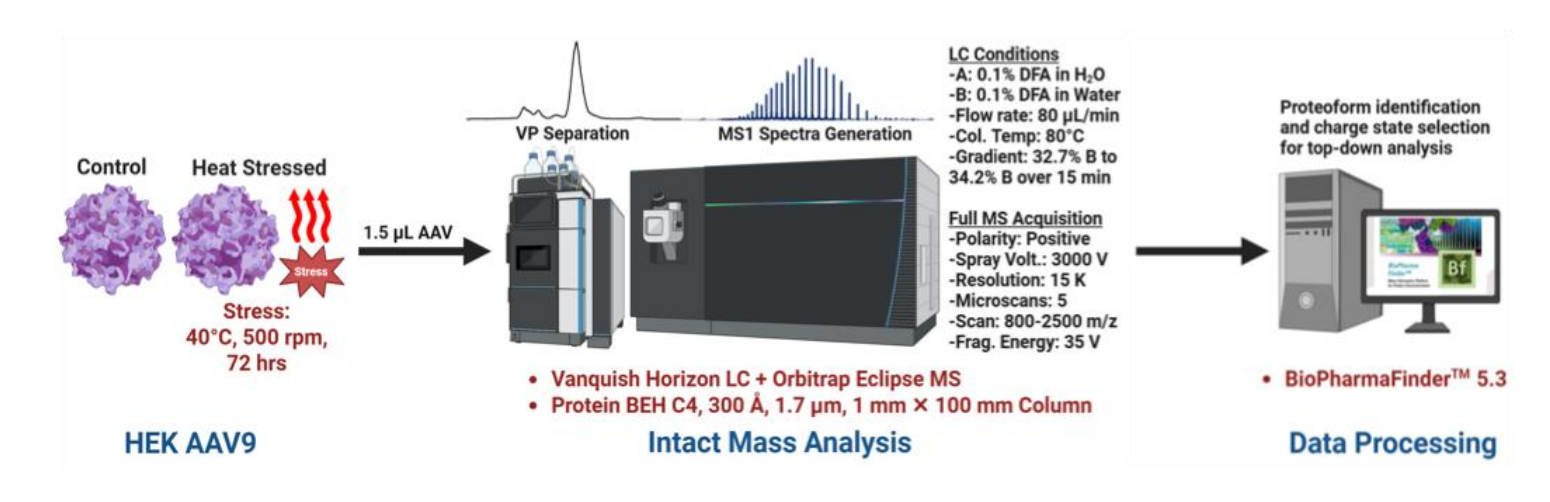
Baculoviral cathepsin

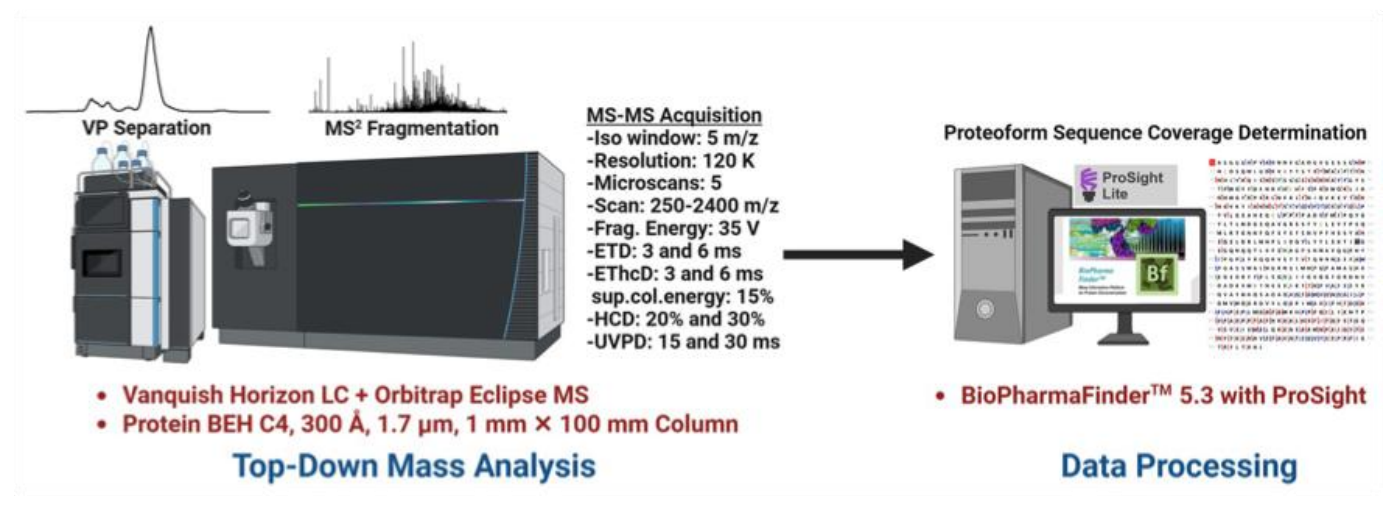
Potential Causes of Fragments

- Immune response
- Acidic conditions



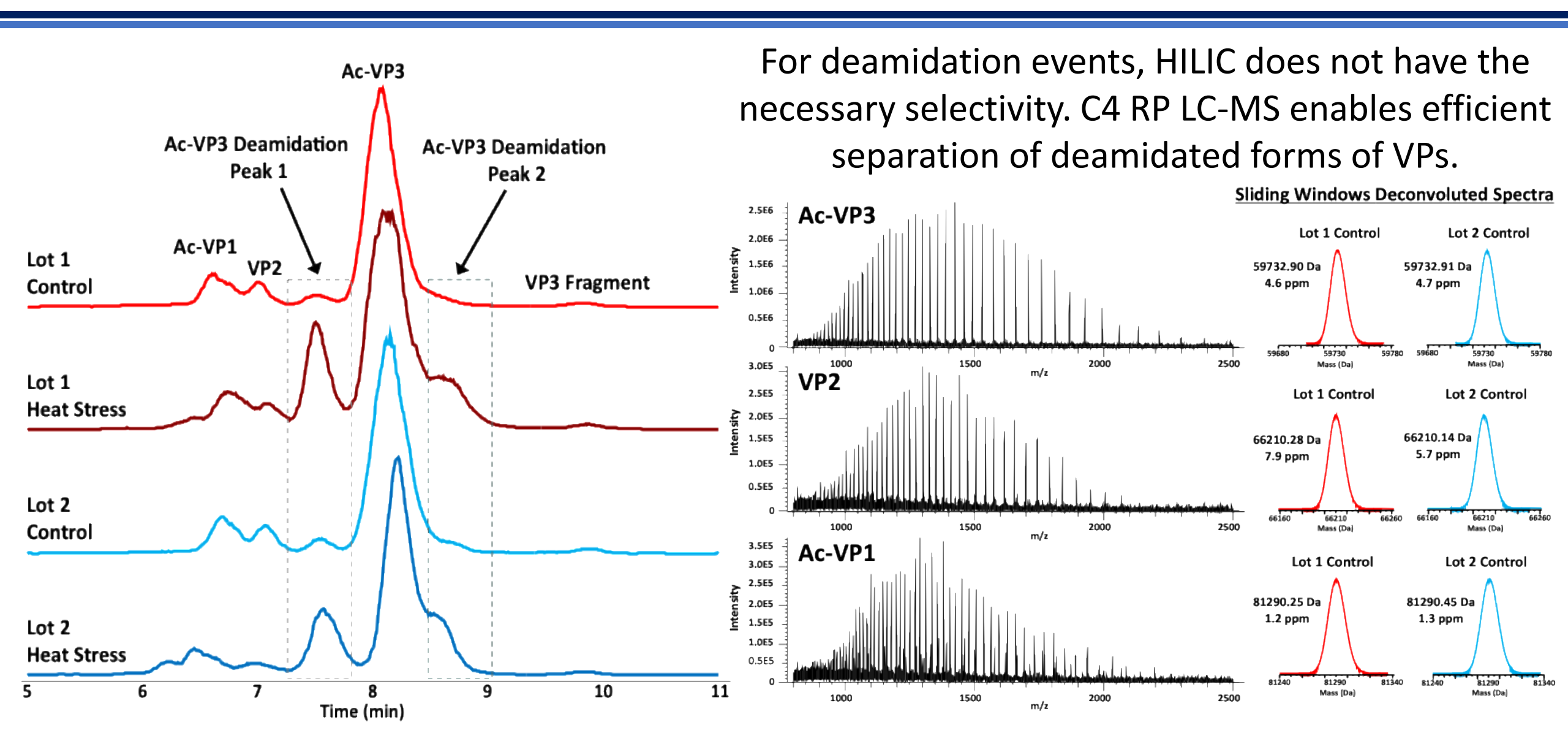
RP LC-MS/MS for Detection of Deamidation Events



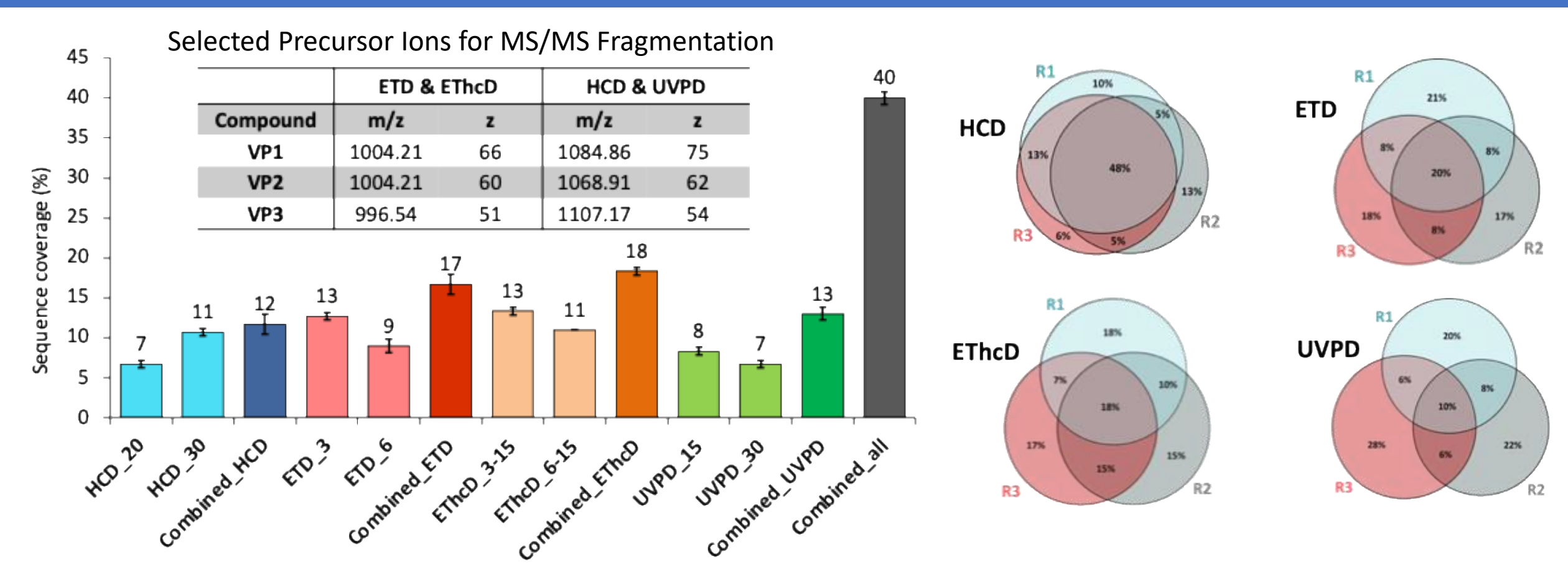


While the HILIC separation of VP's works well, for modifications such as deamidation events, HILIC does not have the necessary selectivity. Reversed-phase separation on C4 enables efficient separation of deamidated forms of the viral proteins.

RP LC-MS/MS for Detection of Deamidation Events

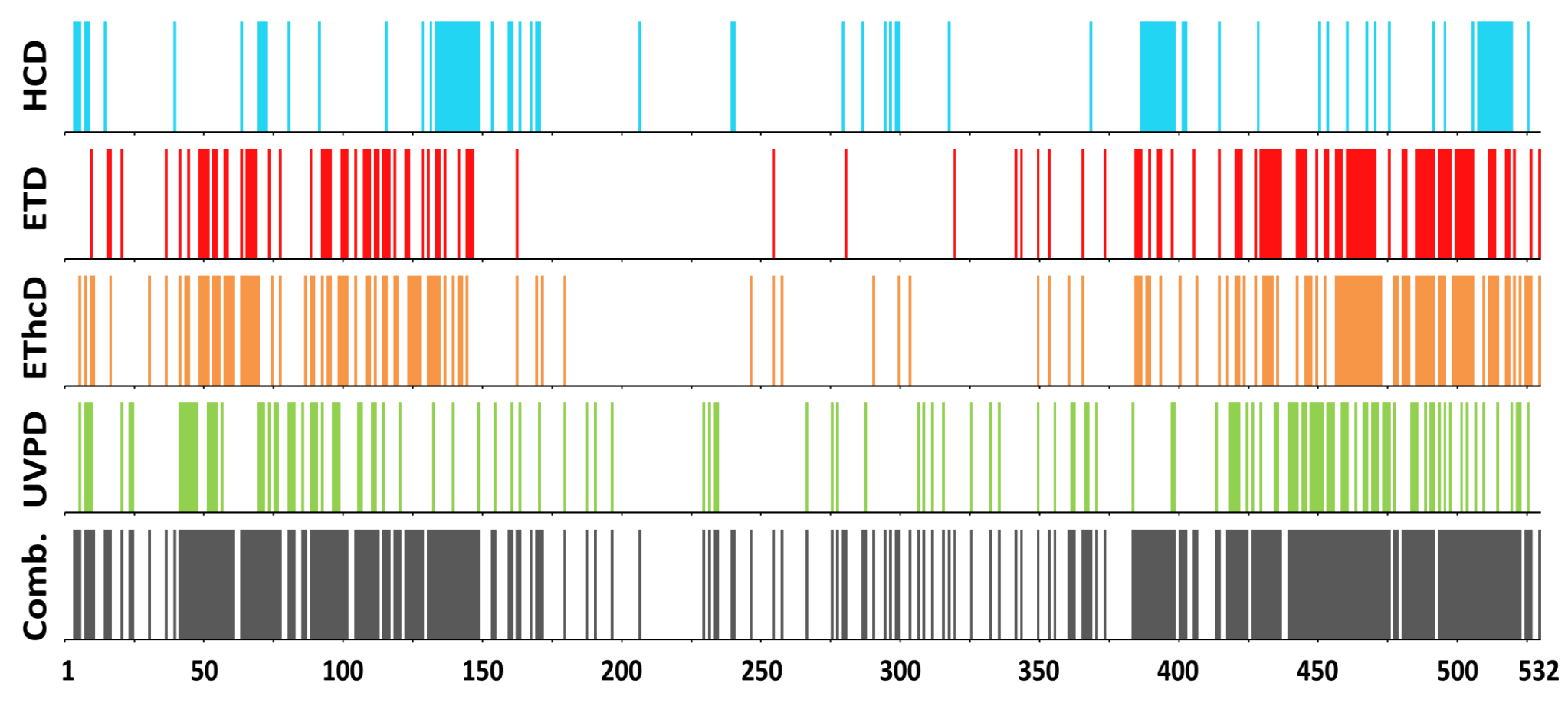


Top-Down LC-MS/MS Using Different Ion Activation



For deamidation events, HILIC does not have the necessary selectivity. C4 RP LC-MS enables efficient separation of deamidated forms of VPs.

Combined Top-Down MS/MS of VP3 on Orbitrap Eclipse

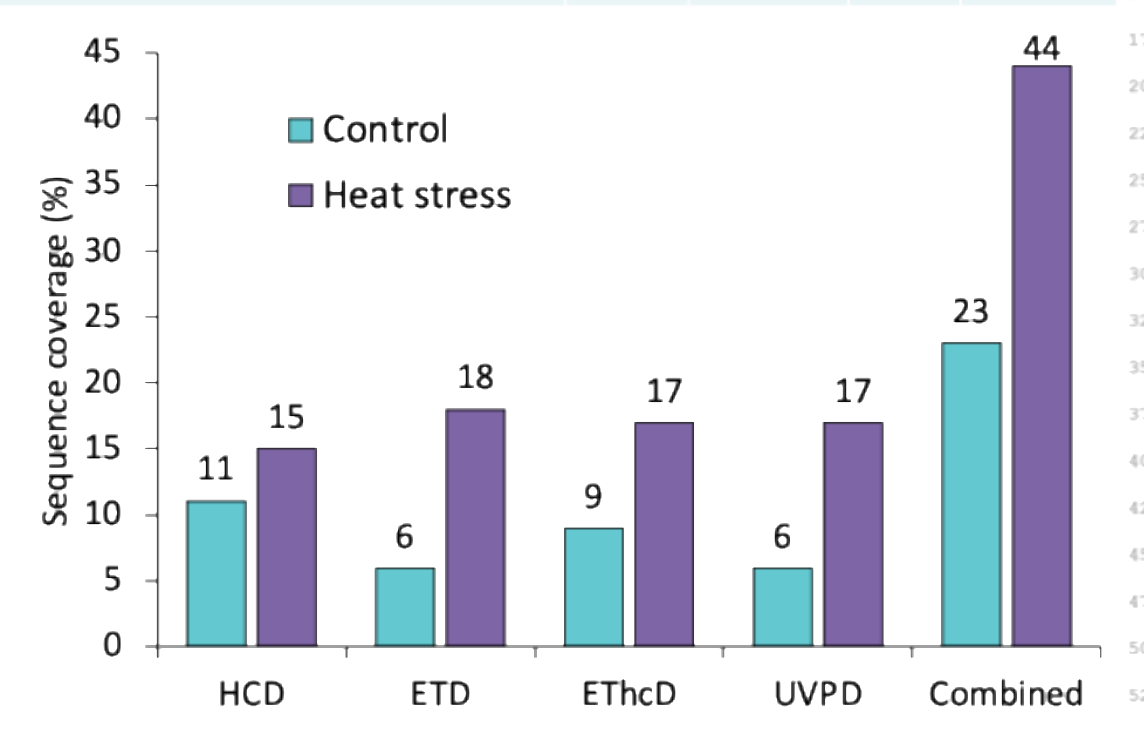


Bar code map depicting the fragmentation location in the amino acid sequence of the fragments detected in all fragmentation strategies using all replicates (n=12).

Top-down MS/MS Data Sequence Map of Deamidated VP3

Residue #	Peptides				Lot 2 Heat Stress (%)
N56+Deamidation (VP1 only)	YLGPGNGLDKGEPVNAADAAALEHDK (Y51-K76); YLGPGNGLDK (Y51-K60); YLGPGNGLDKGEPVNAADAAALEHDKAYDQQLK (Y51-K83)	14.28	41.80	15.87	47.60
N451+Deamidation (VP3:N249)	TINGSGQNQQTLK (T449-K461)	3.15	33.34	8.55	39.97

Peptide mapping identified N249 as a deamidation site. Top-down MS/MS of the Ac-VP3-DP1 peak also enabled identification of the deamidated residue. Overall performance of top-down LC-MS/MS is dependant on the abundance of the proteoform under study.



N A S G G GAP VADON N E G A D GV G SS S G NW 25 26 H C D S Q W L G D R V I T T S T R T W A L P T Y N 50 51 NHL YKOLISINS TIS G G SISINIDINIAIY) FIGIY S 75 16 T)PWGYFDFNRFHCHFSPRDWQRLIN 100 101 NNWG FRP KR LIN F K LIFIN I Q VIK E V TIDIN 125 126 NG VKT I ANNILTSTVQVFTDSDYQLP 150 151 Y V L G S A H E G C L P P F P A D V F M I P Q Y G 175 176 Y L T L N D G S Q A V G R S S F Y C L E Y F P S Q 200 201 M L R T G N N F Q F S Y E F E N V P F H S S Y A H 225 226 S Q S L D R L M N P L I D Q Y L Y Y L S K T I N G 250 251 S G Q N Q Q T L K F S V A G P S N M A V Q G R N Y 275 276 I P G P S Y R Q Q R V S T T V T Q N N N S E F A W 300 301 P G A S S W A L N G R N S L M N P G P A M A S H K 325 326 E G E D R F F P L S G S L I F G K Q G T G R D N V 350 351 DADKVMITNEEEIKLTTNPVATESYG 375 376 Q V A T N H Q S A Q A Q A Q T G W V Q N Q G I L L P 400 401 G M V W Q D R D V Y L Q G P I W A K I P H T D G N 425 426 F H P S P L M G G F G M K H P P Q I L I K N T P 450 451 V[P[A[D[P[P T[A[F]N[K]D[K]L]N[S[F[I]T[Q[Y[S[T[G Q 475] 476 V S V E I E W E L Q K E N S K R W N P E L Q Y T S 500 501 NYYKSNN VEEFALVNITEEGVYYSEEPRIPLI G 525 526 TRYLTRNL





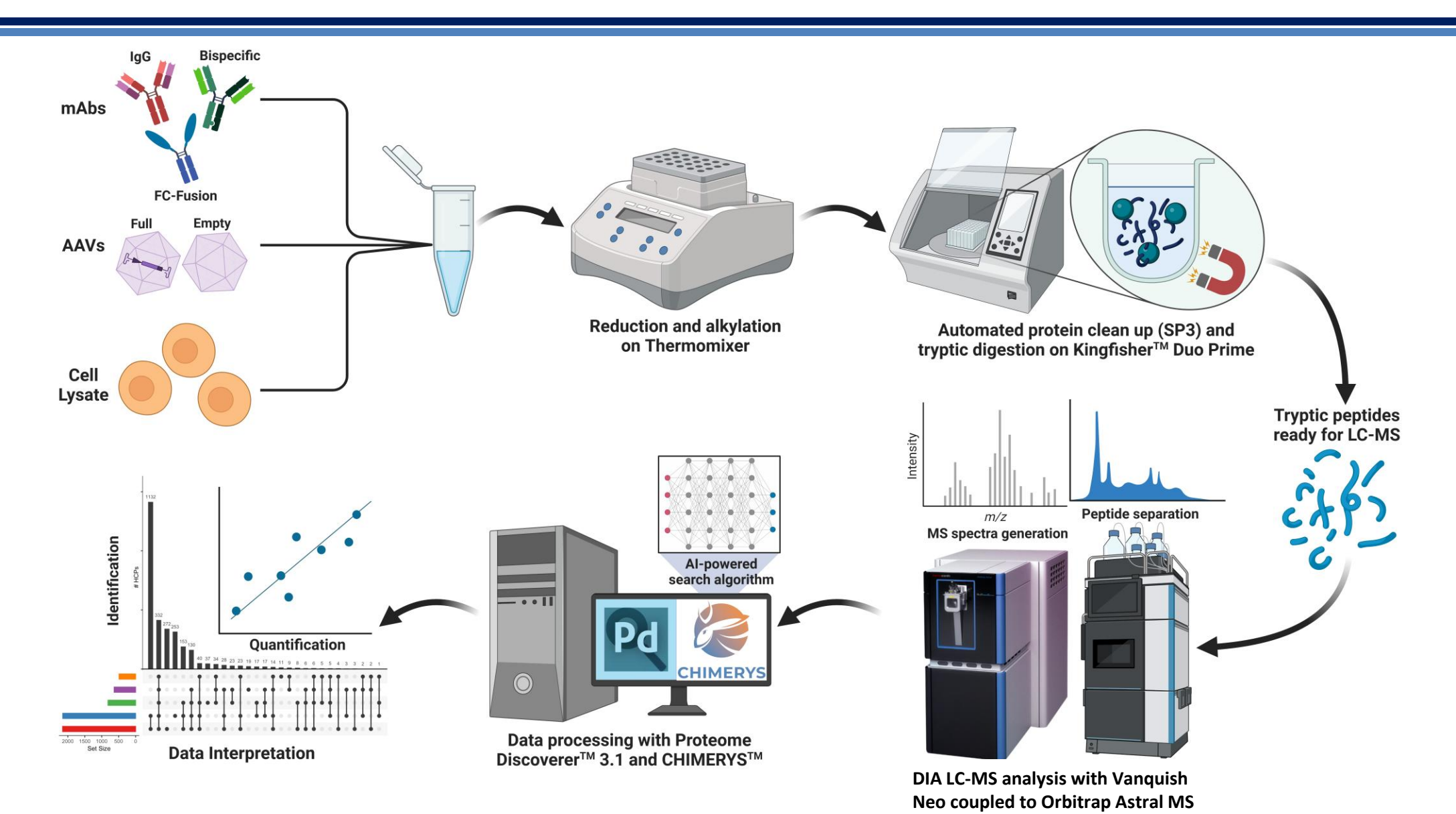
The Thermo Scientific™ Orbitrap™ Astral™ MS - Powered by the synergy of two synchronized HRAM analysers

ORBITRAP ANALYZER for high MS/MS	dynamic range HRAM MS and
HRAM Scan Rate	Up to 40 Hz
Intrascan dynamic range	>5000 with single microscan
Max Resolution	480,000 at <i>m/z</i> 200
Mass Accuracy	RMS <3 ppm
Max <i>m/z</i> range	Up to <i>m/z</i> 8000 with Biopharma Option

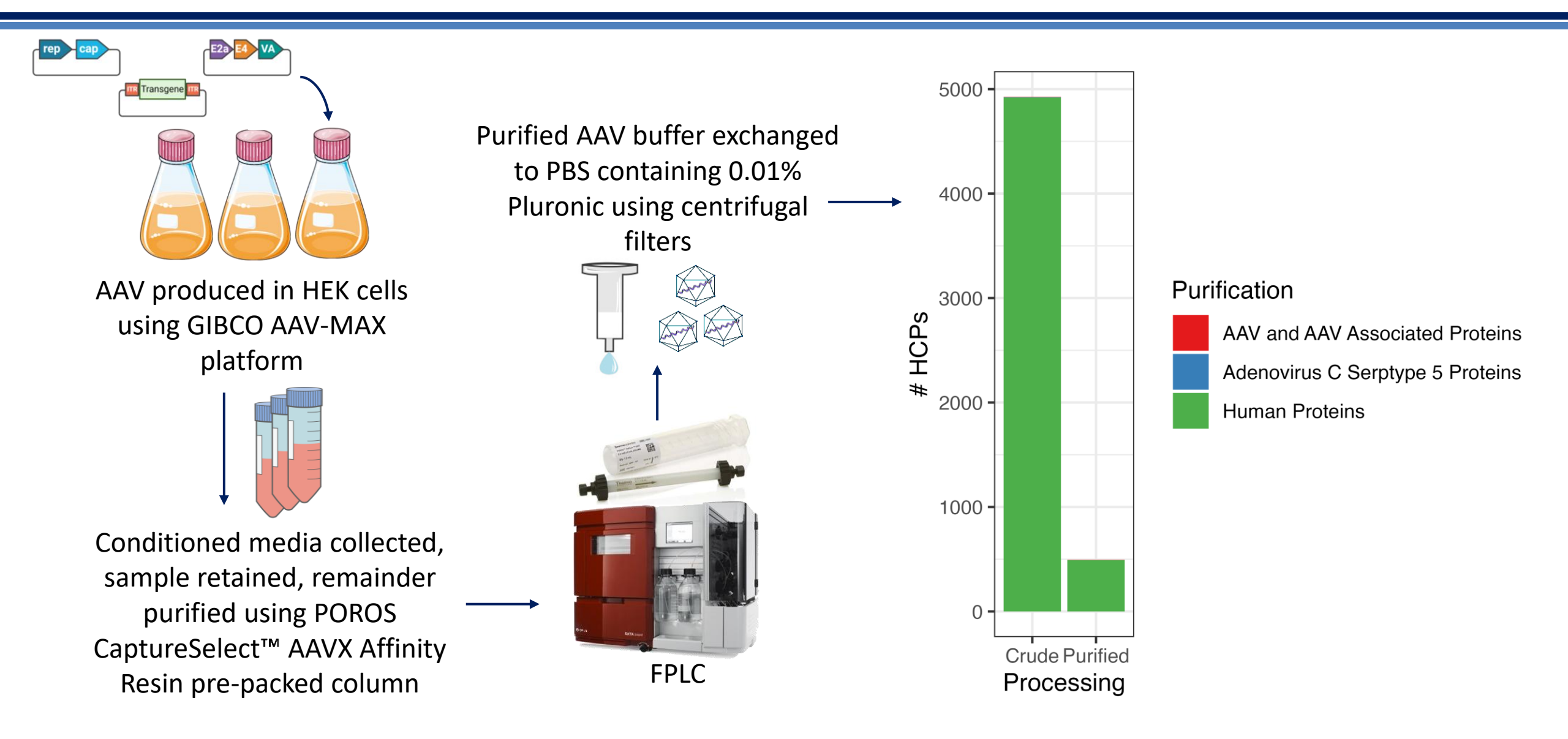


ASTRAL ANALYZER for fast and sensitive high dynamic range HRAM SIM and MS/MS								
Sensitivity	Single ion detection							
HRAM Scan Rate	Up to 200 Hz							
Intrascan dynamic range	>1000 with single microscan							
Resolution	80,000 at <i>m/z</i> 524							
Mass Accuracy	RMS <5 ppm							

Sample Preparation Workflow

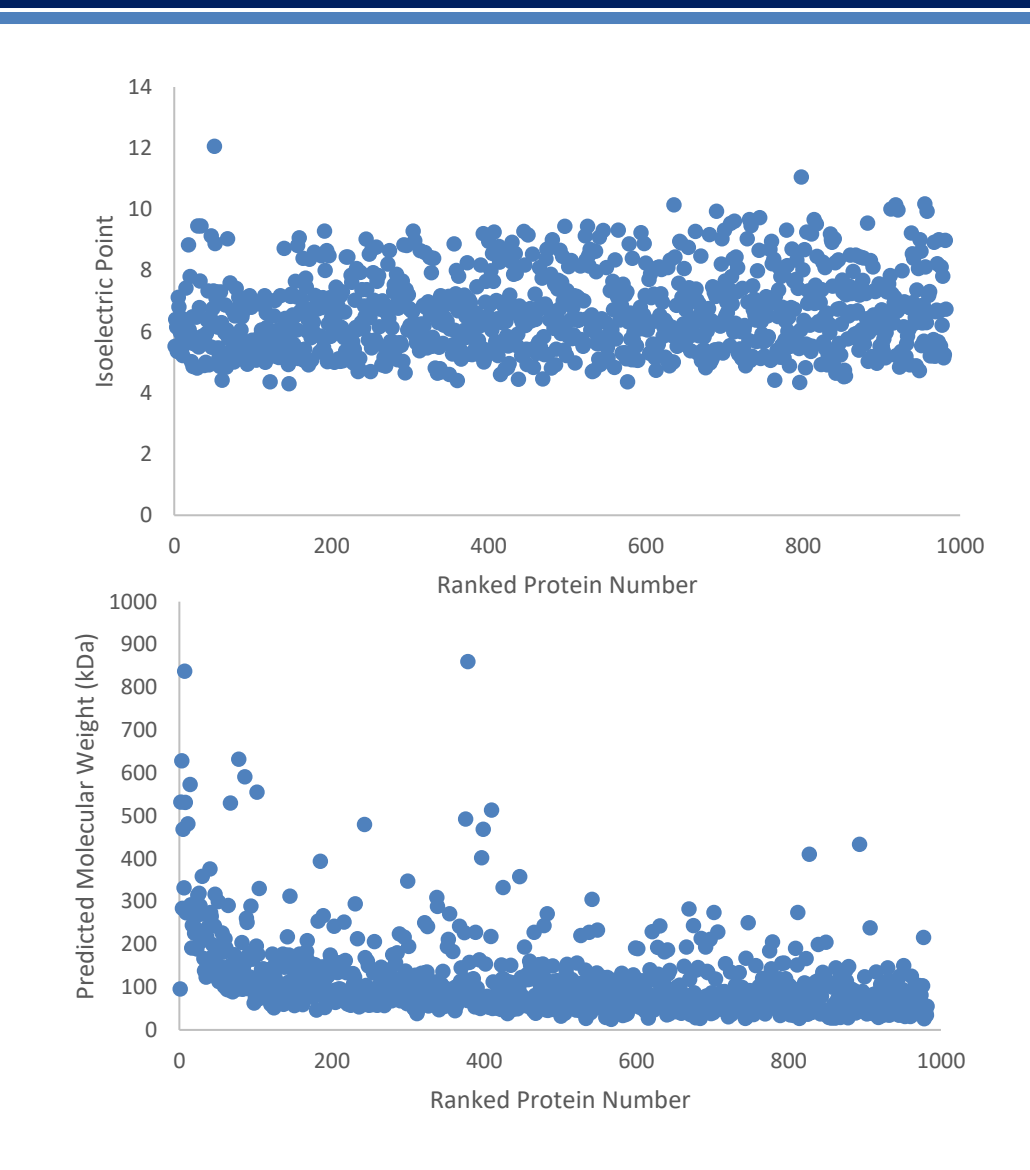


Tracking HCP Clearance using AAVX Affinity Chromatography

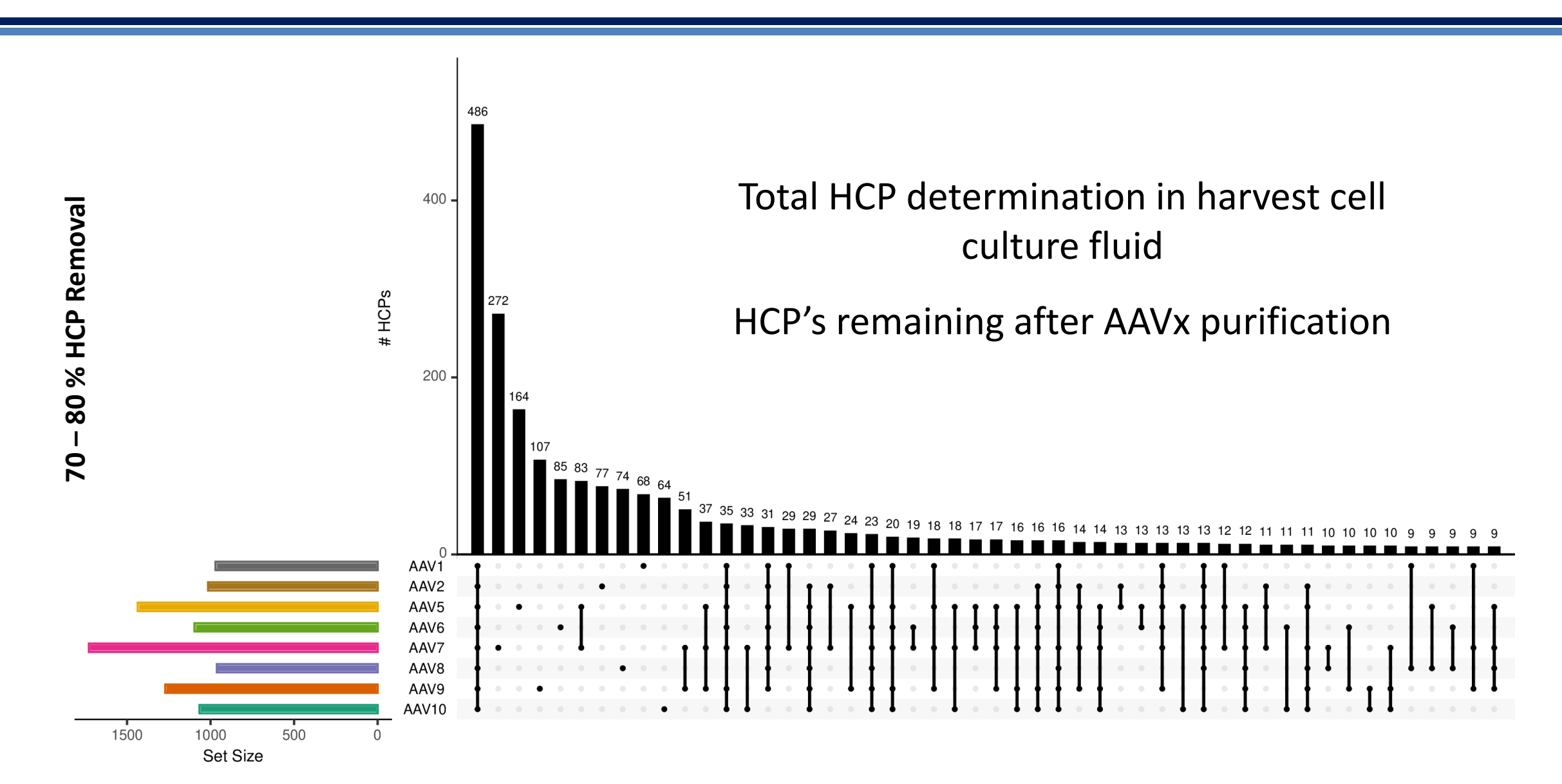


HCPs Associated with Purified CMV-GFP AAV8

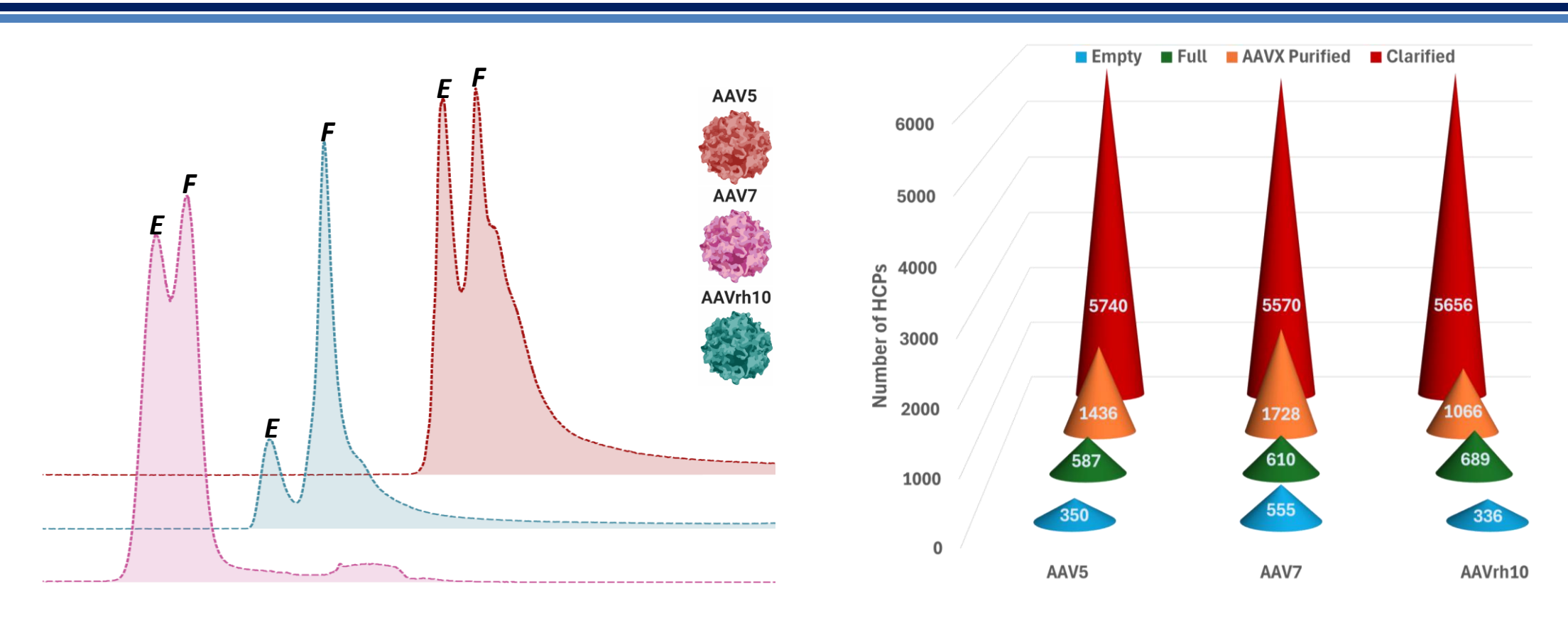
- AAVX purification resulted in ~80% reduction in the levels of HCPs present in the process stream using a simple bind and elute method.
- For proteins associated with the retained viral capsids, GO terms relating to binding, in particular protein binding (92.7% of the total set) were enriched. 97.1% were mapped as being intracellular proteins.
- Standard physiochemical parameters were explored including molecular mass, pl, hydrophobicity etc.
 However, distributions were broad and as expected, no correlation existed.



Exploring HCP Distribution Across Various AAV Serotypes

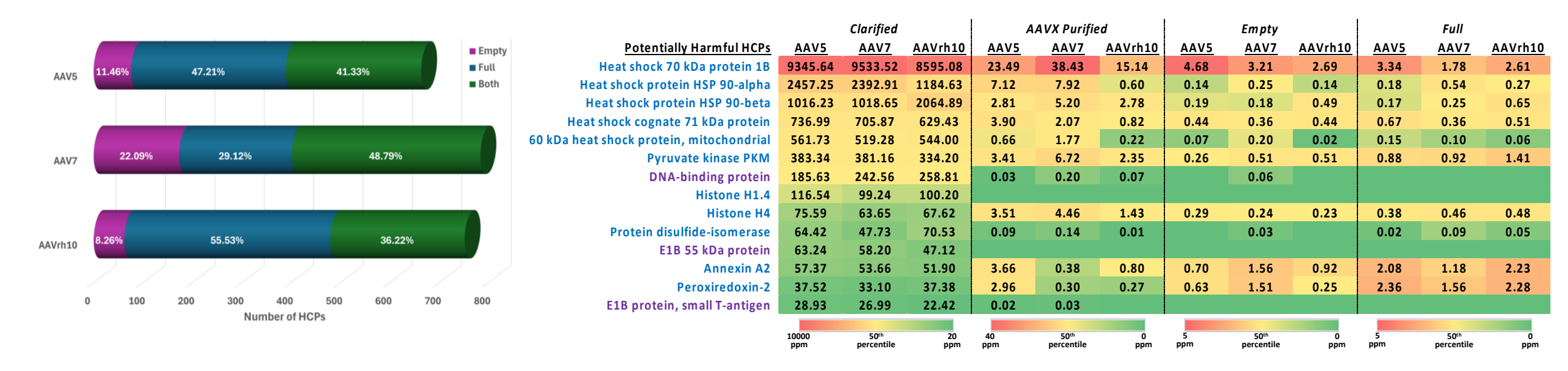


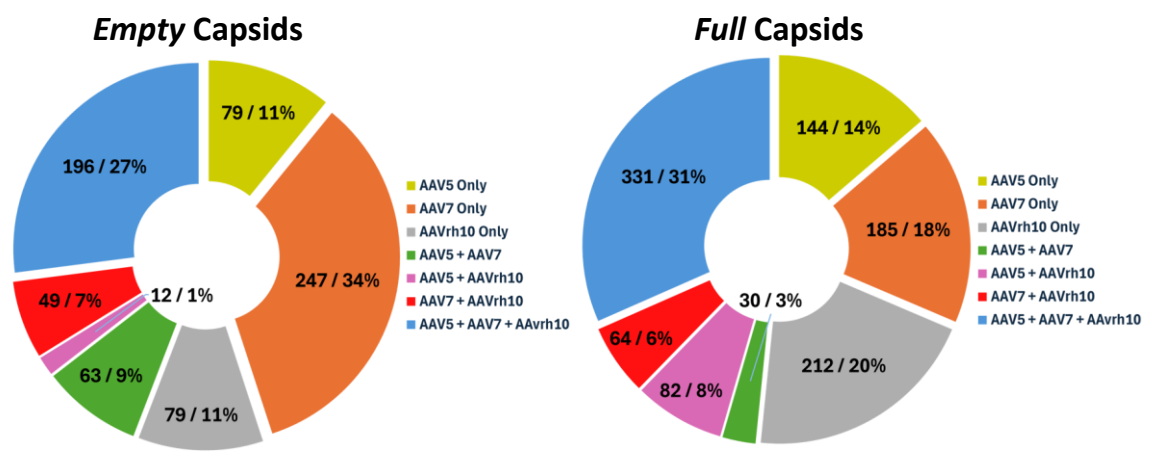
Monitoring Clearance Using Two-Step Downstream Processing



Post AAVX affinity purification, anion exchange separation of empty and full capsids were performed using Poros XQ. Fractions were collected and analysed by LC-MS on Orbitrap Astral to investigate clearance of the HCPs and distribution across the different capsid fill states.

Distribution of HCPs across Empty and Full Capsids





- Ability to separate empty and full capsids affected differentiation of HCP loads, however some specificity was observed.
- Similarly, specificity was observed for the serotypes analysed.
- 'Problematic HCPs' were investigated in the resulting LC-MS data to evaluate their clearance, as shown in the heatmap, the majority were cleared by AAVx affinity chromatography.

Summary

- Native MS and CDMS can be coupled with upfront anion exchange chromatography for confirmation of capsid fill state. Partial capsids not observed either by chromatography or MS, thought to be due to GOI size.
- Viral protein separation possible using various chemistries, HILIC method works well and is simple to deploy, however, reversed-phase outperforms for separation of deamidated forms.
- Top-down MS/MS showing strong potential for VP specific characterisation. Combination of different ion activation strategies on tribrid MS instrument enabled excellent N- and Cterminal fragmentation.
- HCP behaviour investigated using throughout the downstream process for HEK293 derived serotypes using Orbitrap Astral. Some specificity identified based on the serotype and capsid fill state, however, AAVx affinity chromatography enables bulk clearance.



Acknowledgements

Thermo Fisher SCIENTIFIC

NIBRT:

Josh Smith, Corentin Beaumal, Sara Carillo, Aaron Richardson, Felipe Guapo, Colin Clarke, Florian Füssl, Lisa Strasser, Silvia Millán-Martín

Thermo Fisher Scientific:

Eugen Damoc, Anna Pashkova, Kristina Srzentic, Tabiwang N. Arrey, Kai Scheffler, Kelly Broster, David M. Horn, Steve G. Milian, Richard O. Snyder

908 Devices:

Erin Redman





